

# Broad angle and frequency tunable photonic crystal-polarization beam splitter based on negative refraction: Transition from right-handed to left-handed medium

MONIKA RAJPUT, R.K. SINHA

TIFAC – Centre of Relevance and Excellence in Fiber Optics and Optical Communication, Department of Applied Physics, Delhi College of Engineering, Faculty of Technology, University of Delhi, Bawana Road, Delhi-110042, India;  
e-mails: monika\_scholar@yahoo.com, dr\_rk\_sinha@yahoo.com

A new design of a broad angle photonic crystal polarization beam splitter (PhC-PBS) with frequency tunable index of refraction, *i.e.* varying from positive to negative, is presented. Designed PhC-PBS shows transition from right-handed medium (positive index medium) to left-handed medium (negative index medium) with change in normalized frequency from 0.437 to 0.516. The design description includes band structure calculations and equi-frequency contour (EFC) analysis, where direction of refraction is tuned by the frequency and thickness of a slab. The proposed PBS splits transverse electric (TE) polarization in negative direction and transverse magnetic (TM) polarization in positive direction for optical communication windows in the range of 1.31  $\mu\text{m}$  and 1.55  $\mu\text{m}$ . Finite difference time domain (FDTD) method is employed to evaluate left-handed, right-handed transmission and reflection characteristics. High transmission and extinction ratio at wide range of incident angles validate proposed design as an efficient and broad angle PBS based on tunable negative refraction. Demonstration of near- and far-field resonance patterns reveals that proposed structure has the high potential in the design and development of the multiple photonic device applications, *i.e.*, highly directional optical antennas also.

Keywords: negative refraction, photonic crystals, negative index medium, equi-frequency surface, polarization beam splitter, optical antenna.

## 1. Introduction

In recent years, interest has grown in the design and development of artificial structures with unusual material properties that can alter the properties of electromagnetic waves and rule the wave propagation [1–10]. In 1968, VESELAGO [11] investigated the media having both electric permittivity  $\epsilon$  and magnetic permeability  $\mu$

simultaneously negative. In such media, the wave vector  $\mathbf{k}$ , magnetic field vector  $\mathbf{H}$  and electric field vector  $\mathbf{E}$  form a left-handed triplet, where light is allowed to bend in a direction opposite to that of ordinary material. This phenomenon is called negative refraction and materials undergoing this phenomenon are called left-handed materials (LHM). It is noticed that in such a material the wave vector  $\mathbf{k}$  is anti parallel to the Poynting vector. Hence energy propagates against the wave vector and phase is advanced in the propagation direction. One of the most exciting results of LHM is the modified Snell's law. Snell's law is used to calculate the refraction angle of a light beam propagating across the boundary of two media with different positive index and is given by the following formula:  $n_1 \sin \theta_i = n_2 \sin \theta_t$ . If we extend the Snell's law in negative refraction, then the refraction angle  $\theta_t$  will be negative when light beam passes through the interface of left- and right-handed material. This relation reveals that the refracted wave will bend to the same side of the normal. Schematic diagrams of this scenario are shown in Fig. 1. Figure 1 explains the case of negative and positive refraction in detail. When light is bending to the same side of normal (left-hand side), it represents negative refraction and this phenomenon again repeats itself at the second interface, here transmission is called left-handed transmission. However bending of light on the opposite side of the normal (right-hand side) represents positive refraction and transmission is called right-handed transmission.

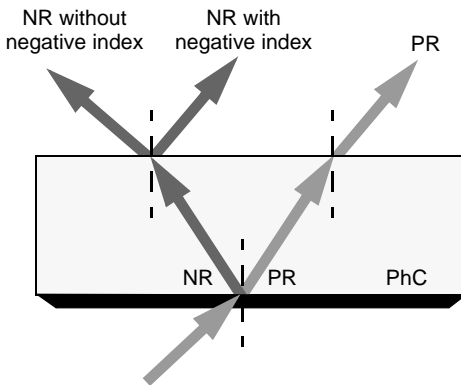


Fig. 1. Schematic of negative refraction (NR) and positive refraction (PR).

After more than 30 years, in 1999 PENDRY *et al.* demonstrated composite structure [12, 13] called metamaterial which consists of rows of split ring resonators and wire strips and the structure shows negative refraction [14]. Recently, it has been shown that similar light behavior, *i.e.*, phenomenon of negative refraction, can be realized in photonic crystals (PhC) [2–4, 15–19] because of their dispersion characteristics and can be analyzed with the help of band structure calculations and dispersion surface analysis [7, 15, 20–22]. Dispersion surfaces are equi-frequency contour (EFC) diagrams of PhC for all allowed propagation vectors at a constant frequency in wave vector space. At a certain frequency, it is possible to get one “or” multiple contours in

the wave vector space. Hence several photonic crystal optical devices based on negative refraction can be designed by utilizing the EFC analysis, band structure calculation, anomalous transmission or diffraction effect [1, 9, 23]. Negative refraction in PhC can be classified in two categories; in the first category, negative refraction occurs in the second and higher order band, *i.e.*, transmission band, while in the second category, negative refraction occurs only in the first band, *i.e.*, partial band gap.

In the present paper, we report the design and analysis of a new structure of photonic crystal polarization beam splitter (PBS) based on negative refraction for optical communication in transmission band. The proposed new design of PBS exhibits negative refraction with high transmission and extinction ratio for a large range of incident angles at two optical communication windows, 1.31  $\mu\text{m}$  and 1.55  $\mu\text{m}$ . It is further shown that with changing the frequency of the transverse electric (TE) polarization of the incident light, the behavior of the structure changes from positive index material to negative index material. Designed structure shows negative refraction without negative index at 1.55  $\mu\text{m}$  while at 1.31  $\mu\text{m}$  material exhibits negative refraction with negative index. Hence, the designed structure exhibits frequency tunable negative refraction for TE polarization, where refractive index shifts from positive to negative when changing frequency. This new design of photonic crystal PBS based on tunable negative refraction works as an efficient and broad angle polarization beam splitter. It is expected that this technique will be useful in the design and development of optical devices and components based on negative refraction.

## 2. Principle and design description

A 2D PhC-PBS, composed of air holes in dielectric  $\varepsilon = 12.4$  (resembling the InAs) with hole radius  $r = 0.3a$ , where  $a$  is lattice constant, is presented. Designed structure shows tunable negative refraction at optical communication wavelengths,  $\lambda = 1.31 \mu\text{m}$  and  $\lambda = 1.55 \mu\text{m}$  for a large range of incident angles.

### 2.1. Negative refraction without negative index

According to dynamical diffraction theory [24], a beam of finite width with incident wave vector  $\mathbf{k}_0$  is incident on a 2D periodic structure. Due to periodicity, a secondary or diffracted wave with the wave vector  $\mathbf{k}_d$  is generated. The wave vector of generated wave ( $\mathbf{k}_d$ ) will be equal to the sum of incident wave vector  $\mathbf{k}_0$  and periodic vector  $\mathbf{K}$ . Hence the Bragg condition gives,

$$\mathbf{k}_d = \mathbf{k}_0 + \mathbf{K}$$

In vacuum, the dispersion surface is a sphere of radius  $\mathbf{k}_0$ . According to transmission geometry of vacuum–PhC interface (Fig. 2), the tangential component of incident wave vector is conserved across the dispersion surface (light-gray sphere). The intersections of this tangential component of the incident wave vector with EFC of PhC (dark-gray sphere) implied the vertices of refracted wave vectors. Figure 2

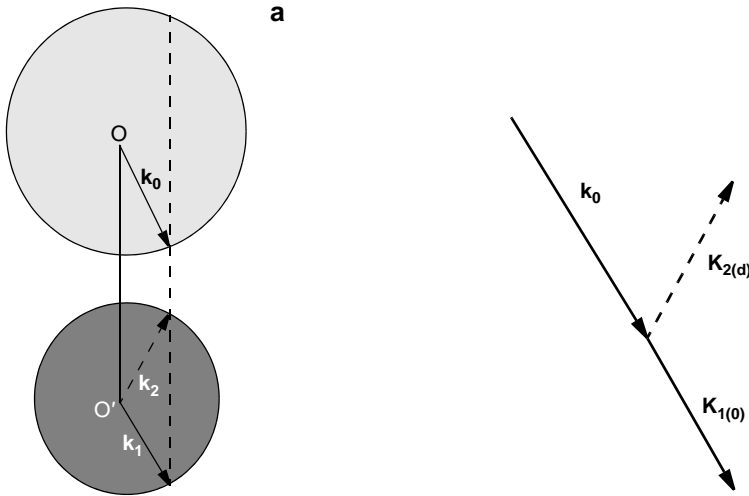


Fig. 2. Vacuum–PhC interface geometry (a) verifies dynamical diffraction theory in PhC (b).

shows two refracted wave vectors pointing in  $\mathbf{k}_1$  and  $\mathbf{k}_2$  directions. If we apply dynamical diffraction theory and suppose these wave vectors correspond to  $\mathbf{k}_0$  and  $\mathbf{k}_d$  wave vectors, then, the index of refraction for  $\mathbf{k}_0$  and  $\mathbf{k}_d$  waves must be different from the average index of refraction.

For these two generated waves, the average direction of energy flow shifts in both directions periodically with change in depth or width of the crystal. Thus dynamical diffraction theory explains that two generated waves undergo coupling and conversion between each other during propagation. A word *Pendellösung* is given by EWALD for this particular phenomenon because of its similarity to energy transfer between two weakly coupled pendulums [24]. Therefore, phase modulation between plane wave components is the origin of Pendellösung effect. Then, the determined wave vector shows a phase modulation  $1/\Lambda$ , where  $\Lambda$  is the modulation period or Pendellösung distance. Dynamical diffraction theory can be used to find the intensity of an outgoing beam in positive and negative direction. The direction of the outgoing beam depends upon the thickness of photonic crystal as a multiple of  $\Lambda$ . Accordingly; if thickness is an even multiple of  $\Lambda/2$ , then output intensity will be maximum in positive direction and if thickness is an odd multiple of half period  $\Lambda/2$ , then output intensity will be maximum in negative direction [25]. The band diagram of our designed structure (Fig. 3a) shows two allowed wave vectors for frequency range  $a/\lambda = 0.425$  to  $0.501$ . The above observation can also be confirmed by the equi-frequency contour diagrams (Fig. 3b) at  $a/\lambda = 0.437$ . Thus in the designed structure, negative refraction can be achieved with varying thickness of a photonic crystal as a multiple of  $\Lambda$ . Pendellösung distances for TE ( $\Lambda_{TE}$ ) and TM ( $\Lambda_{TM}$ ) polarizations are calculated from the band structure diagram of the proposed structure as shown in Fig. 3.

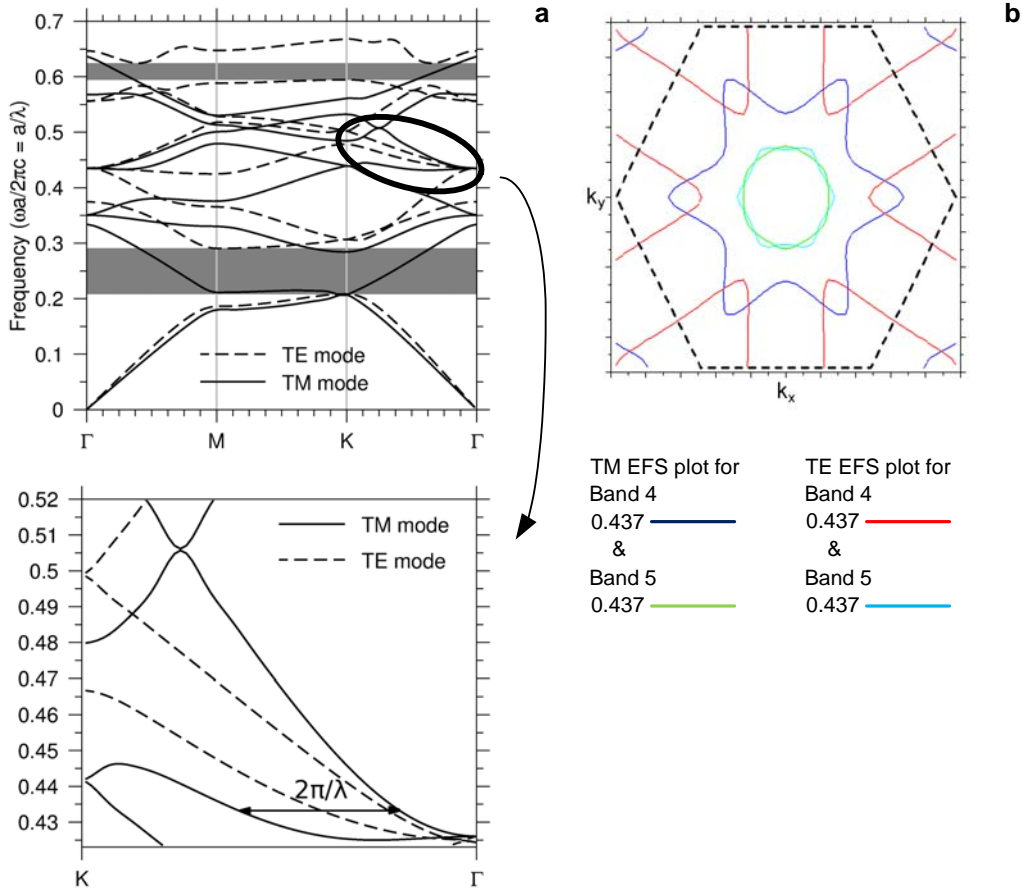


Fig. 3. Band diagram of sample structure, where inset shows multiple wave vectors for a given frequency range (a). EFC plot at  $a/\lambda = 0.437$  lies in a given frequency range confirming the overlapping of different bands (b).

Thickness of photonic crystal can be determined from the following condition:

$$t = \frac{m^* \Lambda_+}{2} = \frac{n^* \Lambda_-}{2}$$

where  $\Lambda_+$  is the Pendellösung distance for the polarization having maximum intensity in positive direction and  $\Lambda_-$  is the Pendellösung distance for the polarization having maximum intensity in negative direction,  $m = 2, 4, \dots$  and  $n = 1, 3, \dots$ . From band structure diagram, we get,  $t = \Lambda_{\text{TM}} = \Lambda_{\text{TE}}/2$ , for  $m = 2, 4, \dots$  and  $n = 1, 3, \dots$ . At  $a/\lambda = 0.437$ ,  $t = 4a$  (here  $a$  is lattice constant) is calculated for the designed structure. For finite difference time domain (FDTD) simulations, we have chosen  $a = 0.677 \mu\text{m}$

at  $a/\lambda = 0.437$  which further corresponds to  $\lambda = 1.55 \mu\text{m}$ . Hence this designed structure refracts TE polarization in negative direction and TM polarization in positive direction. Therefore, it can be used as a PBS based on negative refraction without using negative index.

## 2.2. Negative refraction with negative index

If we now tune the normalized frequency  $a/\lambda = 0.516$ , then the band diagram and the EFC plot of the same designed structure for TE polarization (Figs. 4a and 4b) reveal that:

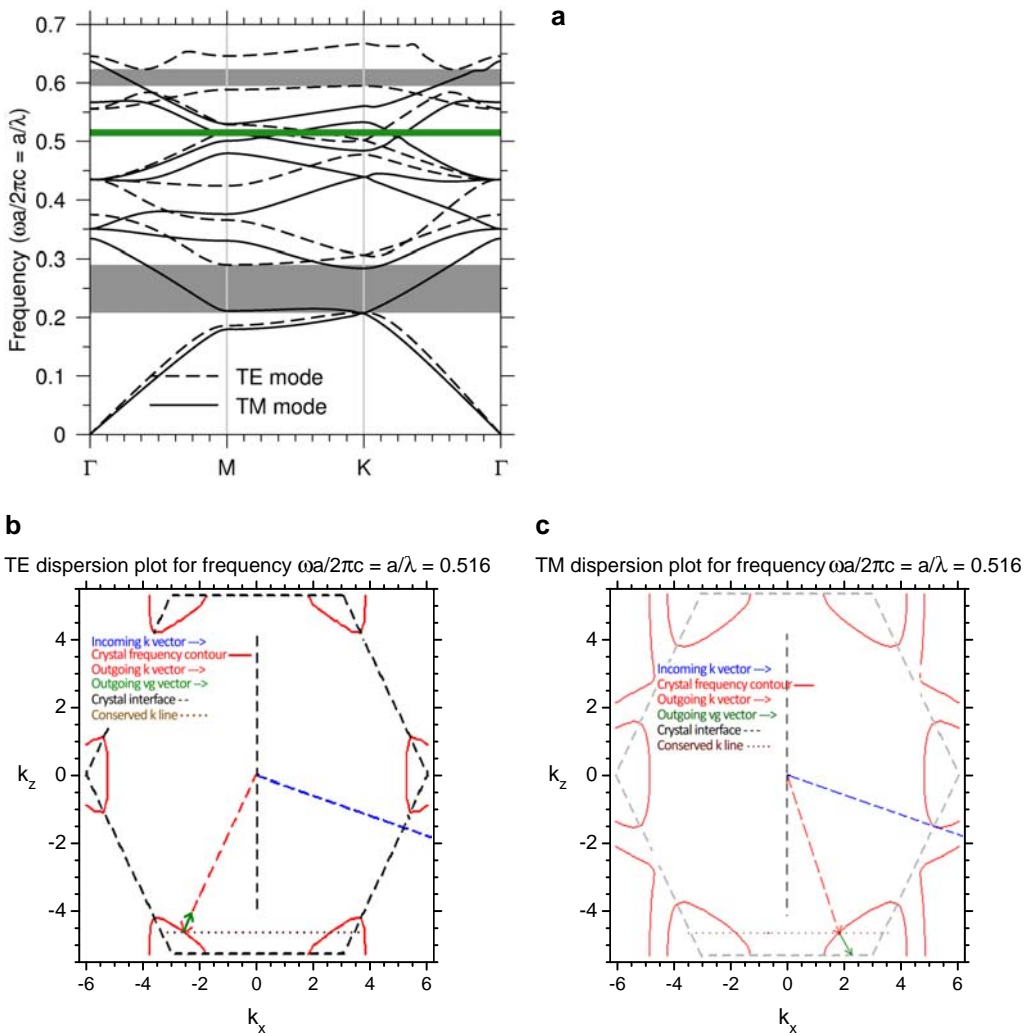


Fig. 4. Band diagram for the designed structure (a). EFC plots for TE polarization (b) and TM polarization (c) at normalized frequency  $a/\lambda = 0.516$ . Green line in (a) represents the region around  $a/\lambda = 0.516$ .

– Group velocity  $\mathbf{v}_g$  points inwards with increasing frequency near the frequency region  $a/\lambda = 0.516$ , hence  $\mathbf{v}_g \cdot \mathbf{k}_f < 0$ , which confirms negative index of refraction, where  $\mathbf{k}_f$  is the refracted propagation wave vector [1].

– Further, from the band structure and the EFC diagram of TM polarization (Fig. 4b), the group velocity  $\mathbf{v}_g$  points outwards, hence  $\mathbf{v}_g \cdot \mathbf{k}_f > 0$ , which confirms positive refraction [1].

The above analysis shows that TE polarization of incident electromagnetic wave exhibits negative index of refraction, while TM polarization suffers positive index of refraction at normalized frequency range  $a/\lambda = 0.516$ . Hence the designed structure can be used as PBS based on negative refraction using negative index. Further, to get greater insight into the electromagnetic response of the designed PhC-PBS, the field map is obtained using FDTD and is shown in Fig. 8. Figure 8 shows the existence of positive refraction for TM polarization and negative refraction for TE polarization. Hence, these FDTD results are in good agreement with those from dispersion analysis of the structure.

### 3. Characterization results

To characterize the performance of proposed PBS, FDTD simulations are carried out for both optical wavelength windows 1.50–1.60  $\mu\text{m}$  and 1.30–1.36  $\mu\text{m}$  for both TE and TM polarizations. Designed PBS works efficiently from the wavelength 1.50  $\mu\text{m}$  to 1.60  $\mu\text{m}$  and from 1.30  $\mu\text{m}$  to 1.34  $\mu\text{m}$  for the desired range of incident angles.

#### 3.1. Negative refraction without negative index

The field map of the designed PBS structure using FDTD simulation is shown in Fig. 5. Here, the incident wave of the wavelength 1.55  $\mu\text{m}$  impinges at an angle  $30^\circ$  on a designed structure of PhC with hexagonal lattice of air holes in InAs with  $r/a = 0.3$  and  $a = 0.677 \mu\text{m}$ . The obtained results show positive refraction of TM polarization (Fig. 5a) and negative refraction of TE polarization (Fig. 5b).

Further, Fig. 6a indicates the normalized intensity spectrum of a refracted beam as a function of the incident angle at the wavelength 1.55  $\mu\text{m}$ . Figure 6b represents

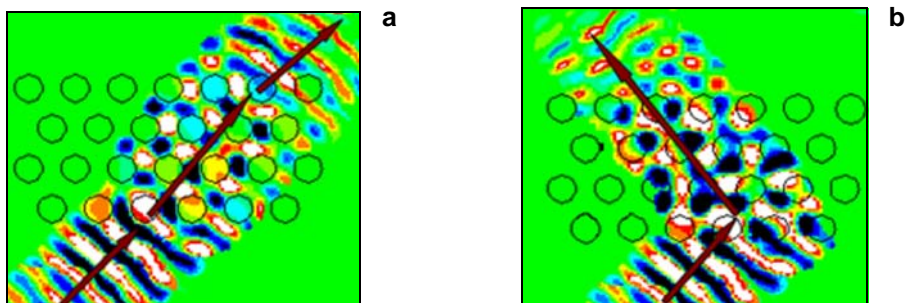


Fig. 5. FDTD results show, positive refraction for TM polarization (a) and negative refraction for TE polarization (b), at an incident angle  $30^\circ$  for wavelength 1.55  $\mu\text{m}$ .

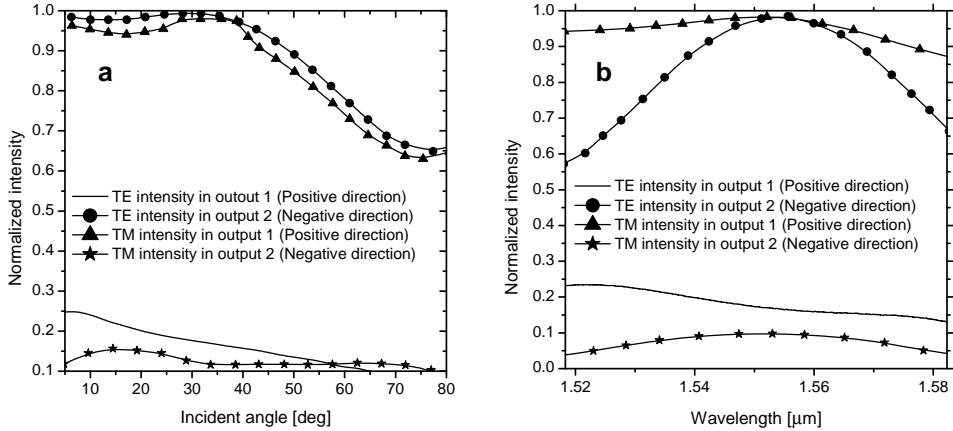


Fig. 6. Normalized intensity of polarization splitter for a range of incident angle  $5-80^\circ$  at  $\lambda = 1.55 \mu\text{m}$  (a), and a range of wavelength varying from  $1.50-1.60 \mu\text{m}$  at an angle of  $30^\circ$  (b).

the normalized intensity spectrum for the wavelength range  $1.50-1.60 \mu\text{m}$  at a particular angle (*i.e.*,  $30^\circ$ ) for positive and negative refractive intensities with both TE and TM polarization, respectively. It is observed from Figs. 6a and 6b that the maximum normalized intensity for TE polarization is obtained from negative direction (output 2) and TM polarization is obtained from positive direction (output 1).

Efficiency of the designed PBS is confirmed by the extinction ratios for TE and TM polarizations. Hence the extinction ratios  $ER_-$  and  $ER_+$  are defined as:

$$ER_- = 10 \log \frac{\text{Transmitted power of TE polarization in output 2}}{\text{Transmitted power of TM polarization in output 2}}$$

$$ER_+ = 10 \log \frac{\text{Transmitted power of TM polarization in output 1}}{\text{Transmitted power of TE polarization in output 1}}$$

Figure 7a shows the angle dependence of an extinction ratio at  $\lambda = 1.55 \mu\text{m}$ . The FDTD simulation indicates that  $ER_- = 19 \text{ dB}$  can be achieved for the incident angle  $40^\circ$  and  $ER_+ = 25 \text{ dB}$  can be achieved for the incident angle of  $30^\circ$ . However, for the fixed value of the incident angle of  $30^\circ$ , variation in an extinction ratio with the wavelength is plotted in Fig. 7b. It is observed from Fig. 7b that  $ER_- = 11 \text{ dB}$  and  $ER_+ = 25 \text{ dB}$  is achieved at  $\lambda = 1.55 \mu\text{m}$  for the designed PBS with an incident angle of  $30^\circ$ .

### 3.2. Negative refraction with negative index

Further, to get greater insight into an electromagnetic response of the designed PhC-PBS at the wavelength of  $1.31 \mu\text{m}$ , the field map is shown in Fig. 8. Here, the incident wave



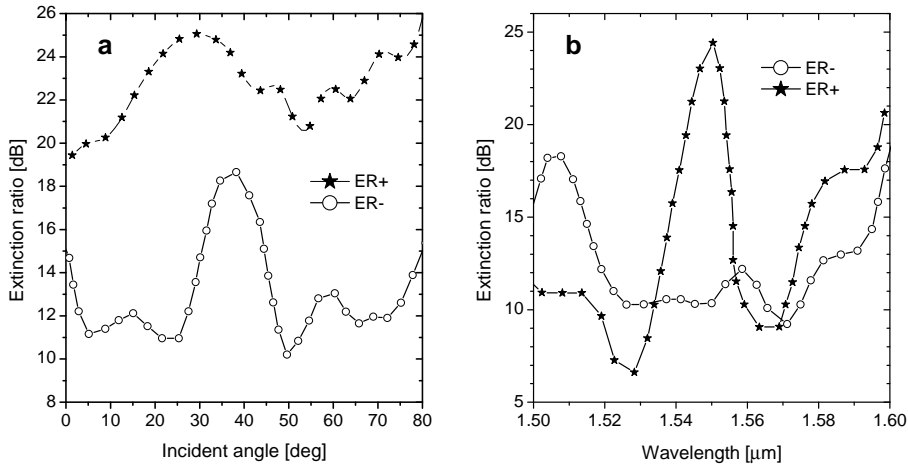


Fig. 7. Angle dependence of extinction ratios,  $ER_-$  and  $ER_+$ , for a range of incident angles  $5^\circ$ – $80^\circ$  at  $\lambda = 1.55 \mu\text{m}$  (a). Wavelength dependence of extinction ratios,  $ER_-$  and  $ER_+$ , at incident angle  $30^\circ$  (b).

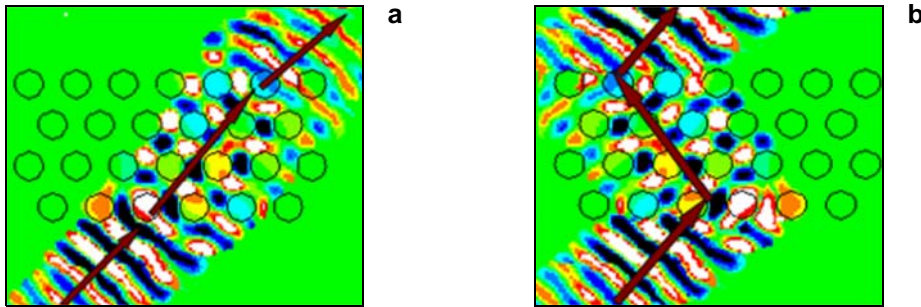


Fig. 8. FDTD results for the incident wave of wavelength  $1.31 \mu\text{m}$  that impinges at an angle  $30^\circ$  over a PhC hexagonal lattice of air holes in InAs with  $r/a = 0.3$ ,  $a = 0.677 \mu\text{m}$ . Positive refraction for TM polarization (a) and negative refraction for TE polarization (b).

of the wavelength of  $1.31 \mu\text{m}$  impinges at an angle  $30^\circ$  on a designed structure of PhC with hexagonal lattice of air holes in InAs with  $r/a = 0.3$  and  $a = 0.677 \mu\text{m}$ . The FDTD results show that positive refraction is achieved for TM polarization (Fig. 8a) and negative refraction is achieved for TE polarization (Fig. 8b). In the FDTD simulation we have taken,  $a = 0.677 \mu\text{m}$  at  $a/\lambda = 0.516$  which corresponds to the wavelength  $\lambda = 1.31 \mu\text{m}$ . The normalized intensity spectrum from the two outputs for both polarizations is shown in Fig. 9a. Figure 9b reveals the wavelength dependence of extinction ratio for a given wavelength range of  $1.3$ – $1.36 \mu\text{m}$ . From Fig. 9b, it is observed that  $ER_- = 19 \text{ dB}$  and  $ER_+ = 21 \text{ dB}$  for  $\lambda = 1.31 \mu\text{m}$ .

Figure 10 is the far-field spectrum, obtained by employing 3D FDTD method for input Gaussian profile. Angular distribution of intensity at the output of the designed

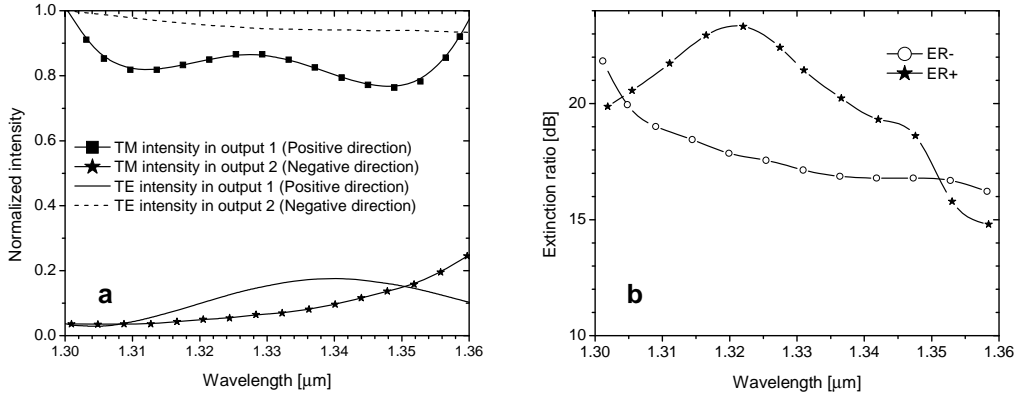


Fig. 9. Normalized intensity spectrum (a) and wavelength dependence of extinction ratios  $ER_-$  and  $ER_+$  (b), of designed PBS in the wavelength range 1.3 μm to 1.36 μm at an incident angle  $30^\circ$ .

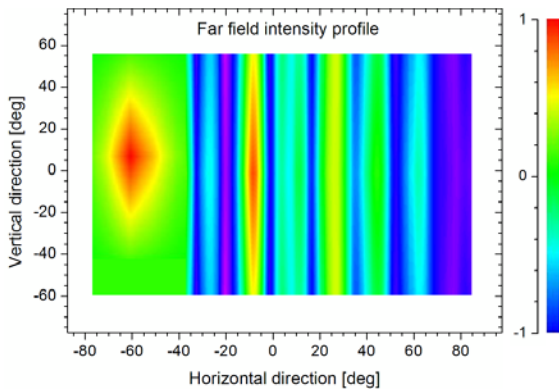


Fig. 10. Far-field intensity pattern of TE mode at  $\lambda = 1.31 \mu\text{m}$ , which shows highly directional negative refraction for designed PhC-PBS.

PhC-PBS for TE polarization is shown in Fig. 10. It is observed that the transmission peak is obtained on the deep negative side (same side to the normal of second interface), which confirms left-handed transmission from the proposed PhC-PBS. The obtained far-field intensity spectrum also confirms highly left-handed directional emission and a strong potential to be used as a directional optical antenna.

## 4. Conclusions

We have proposed a new design of a frequency tunable photonic crystal based on negative refraction and its application as an enhanced PBS device at optical communication windows, 1.31 μm and 1.55 μm. By combining the dynamical diffraction theory, band diagram calculations and EFC analysis in the designed structure, a broad angle PBS is achieved. The designed structure exhibits enhanced

transmission and extinction ratio (up to 24 dB) at much larger range of the incident angle region ( $0^\circ$ – $80^\circ$ ) at an optical communication window. Far-field spectrum is also obtained and confirmed highly directional left-handed transmission from the proposed PhC-PBS, which confirms its multiple photonic device applications potential.

*Acknowledgements* – The authors gratefully acknowledge the initiatives and support towards the establishment of TIFAC – Centre of Relevance and Excellence in Fiber Optics and Optical Communication at Delhi College of Engineering, Delhi through Mission REACH program of Technology Vision – 2020, Government of India.

## References

- [1] RAJPUT M., SINHA R.K., *All-angle negative refraction for visible light from left-handed metallo-dielectric photonic crystal: theoretical and numerical demonstration with nanophotonic device application*, Applied Physics B **98**(1), 2010, pp. 99–106.
- [2] JOANNOPOULOS J.D., VILLENEUVE P.R., FAN S., *Photonic crystals: Putting a new twist on light*, Nature (London) **386**, 1997, pp. 143–149.
- [3] YANG S.Y., WU J.Y., HORNG H.E., HONG C.Y., YANG H.C., *Direct observation for superprism effect in photonic crystals utilizing negative refraction*, Journal of Applied Physics **103**(5), 2008, p. 053110.
- [4] CUBUKCU E., AYDIN K., OZBAY E., FOTEINOPOULOU S., SOUKOULIS C.M., *Electromagnetism waves: Negative refraction by photonic crystals*, Nature (London) **423**, 2003, pp. 604–605.
- [5] SINHA R.K., RAWAL S., *Modeling and design of 2D photonic crystal based Y-type dual band wavelength demultiplexer*, Optical and Quantum Electronics **40**(9), 2008, pp. 603–613.
- [6] BABA T., ASATSUMA T., MATSUMOTO T., *Negative refraction in photonic crystals*, MRS Bulletin **33**(10), 2008, pp. 927–930.
- [7] XIANYU AO, LIU LIU, WOSINSKI L., SAILING HE, *Polarization beam splitter based on a two-dimensional photonic crystal of pillar type*, Applied Physics Letters **89**(17), 2006, p. 171115.
- [8] MOCCELLA V., DARDANO P., MORETTI L., RENDINA I., *A polarizing beam splitter using negative refraction of photonic crystals*, Optics Express **13**(19), 2005, pp. 7699–7707.
- [9] KIM H.J., Q-HAN PARK, HEONSU JEON, YOUNGHO CHOE, *Photonic crystal superprism based on negative refraction*, Journal of the Korean Physical Society **49**(3), 2006, p. 923.
- [10] FARHAT M., GUENNEAU S., MOVCHAN A.B., ENOCH S., *Achieving invisibility over a finite range of frequencies*, Optics Express **16**(8), 2008, pp. 5656–5661.
- [11] VESELAGO V.G., *The electrodynamics of substances with simultaneously negative values of  $\epsilon$  and  $\mu$* , Soviet Physics Uspekhi **10**(4), 1968, pp. 509–514.
- [12] PENDRY J.B., HOLDEN A.J., ROBBINS D.J., STEWART W.J., *Magnetism from conductors and enhanced nonlinear phenomena*, IEEE Transactions on Microwave Theory and Techniques **47**(11), 1999, pp. 2075–2084.
- [13] PENDRY J.B., HOLDEN A.J., STEWART W.J., YOUNGS I., *Extremely low frequency plasmons in metallic mesostructures*, Physical Review Letters **76**(25), 1996, pp. 4773–4776.
- [14] SHELBY R.A., SMITH D.R., SCHULTZ S., *Experimental verification of a negative index of refraction*, Science **292**(5514), 2001, pp. 77–79.
- [15] PENDRY J.B., *Negative refraction*, Contemporary Physics **45**(2), 2004, pp. 191–202.
- [16] PENDRY J.B., *Negative refraction makes a perfect lens*, Physical Review Letters **85**(18), 2000, pp. 3966–3969.
- [17] NOTOMI M., *Theory of light propagation in strongly modulated photonic crystal: Refraction like behavior in the vicinity of photonic band gap*, Physical Review B **62**(16), 2000, pp. 10696–10705.

- [18] PARIMI P.V., LU W.T., VODO P., SOKOLOFF J., DEROV J.S., SRIDHAR S., *Negative refraction and left-handed electromagnetism in microwave photonic crystals*, Physical Review Letters **92**(12), 2004, p. 127401.
- [19] HUANG Y.J., LU W.T., SRIDHAR S., *Alternative approach to all-angle-negative-refraction in two-dimensional photonic crystals*, Physical Review A **76**(1), 2007, p. 013824.
- [20] LUO C., JOHNSON S.G., JOANNOPOULOS J.D., *All-angle negative refraction in a three-dimensionally periodic photonic crystal*, Applied Physics Letters **81**(13), 2002, pp. 2352–2354.
- [21] GUVEN K., AYDIN K., ALICI K.B., SOUKOULIS C.M., OZBAY E., *Spectral negative refraction and focusing analysis of two-dimensional left-handed photonic crystal lens*, Physical Review B **70**(20), 2004, p. 205125.
- [22] MIN QIU, THYLEN L., SWILLO M., JASKORZYNSKA B., *Wave propagation through a photonic crystal in a negative phase refractive-index region*, IEEE Journal of Selected Topics in Quantum Electronics **9**(1), 2003, pp. 106–110.
- [23] MOMENI B., HUANG J., SOLTANI M., ASKARI M., MOHAMMADI S., RAKHSHANDEHROO M., ADIBI A., *Compact wavelength demultiplexing using focusing negative index photonic crystal superprisms*, Optics Express **14**(6), 2006, pp. 2413–2422.
- [24] EWALD P.P., *Crystal optics for visible light and X rays*, Reviews of Modern Physics **37**(1), 1965, pp. 46–56.
- [25] MOCELLA V., *Negative refraction in photonic crystals: Thickness dependence and Pendellösung phenomenon*, Optics Express **13**(5), 2005, pp. 1361–1367.

*Received May 6, 2010  
in revised form August 12, 2010*